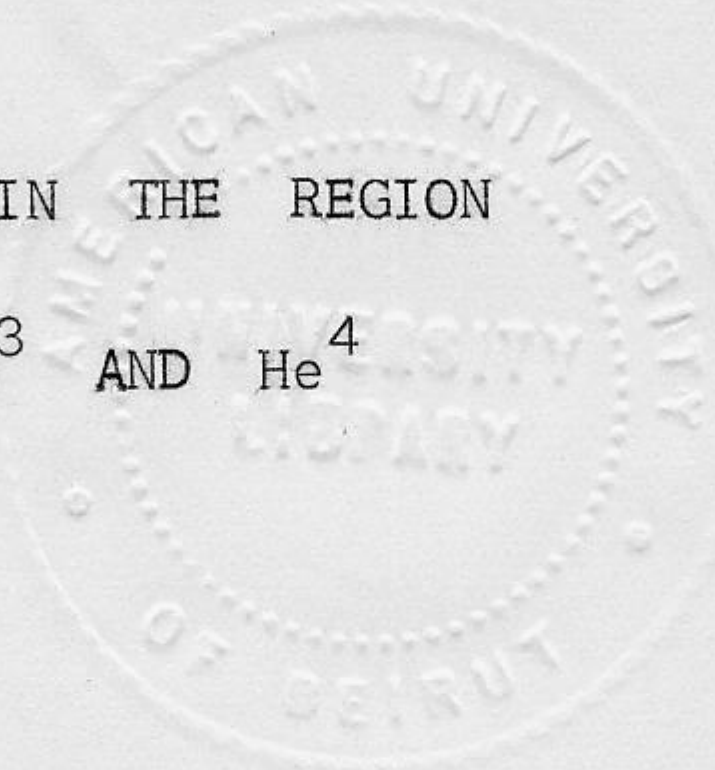


丁  
1029  
0.1

SOME COMMENTS ON PVT MEASUREMENTS IN THE REGION  
NEAR THE CRITICAL POINT FOR He<sup>3</sup> AND He<sup>4</sup>



by

Layla GHUNAYM

SUBMITTED IN PARTIAL FULFILMENT OF THE REQUIREMENTS FOR THE DEGREE  
OF MASTER OF SCIENCE IN THE PHYSICS DEPARTMENT  
OF THE SCHOOL OF ARTS AND SCIENCES,  
AMERICAN UNIVERSITY OF BEIRUT  
BEIRUT, LEBANON

BEIRUT, August 1968.

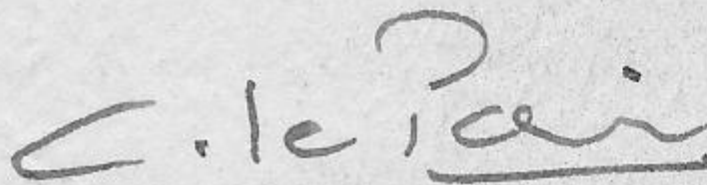
SOME COMMENTS ON PVT MEASUREMENTS IN THE REGION

NEAR THE CRITICAL POINT FOR He<sup>3</sup> AND He<sup>4</sup>

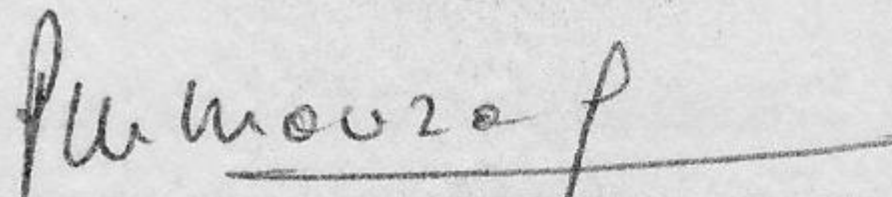
by

Layla GHUNAYM

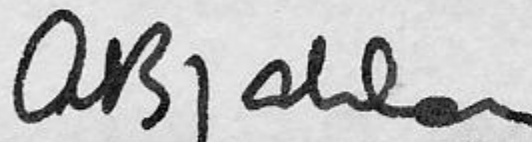
Approved:



Advisor: Dr. C. le Pair, Assistant Professor of Physics



Member of Committee: Dr. P. Mourad, Assistant Professor of Physics



Member of Committee: Dr. A.B. Zahlan, Professor of Physics

AUGUST, 1968.

SOME COMMENTS ON PVT MEASUREMENTS IN THE REGION  
NEAR THE CRITICAL POINT FOR He<sup>3</sup> AND He<sup>4</sup>

GHUNAYM

## ACKNOWLEDGEMENTS

The author is grateful for the technical help of the Physics Mechanical and Glass Workshops staff, in particular Mr. George Boyadjian, Mr. Amin Halabi and Mr. Daoud Srouji.

Thanks are also due to Mr. Pierre Jamous for typing this thesis, and to Mr. George Majdalani for his neat reproduction of the figures.

## A B S T R A C T

A general review of the theories concerning the critical region is presented. The major experimental results of PVT measurements in this region are discussed in particular for He<sup>3</sup> and He<sup>4</sup>. Finally an experimental technique is described. This technique makes possible simultaneous measurements of Pressure, Volume and Temperature of a fixed sample mass. The volume changes would be observed by the variation of the inductance of a coil.

TABLE OF CONTENTS

	Page
ABSTRACT .....	iv
LIST OF FIGURES .....	vi
I. INTRODUCTION .....	1
II. THEORY .....	7
III. EXPERIMENTAL .....	38

## LIST OF FIGURES

Figure		Page
1	The Phase Equilibrium Curve .....	3
2	The Densities of Saturated Liquid and Saturated Vapor, showing the rectilinear Diameter .....	6
3	Schematic Isotherms for a Simple Fluid in the Critical Region .....	9
4	Schematic Isotherm for a van der Waals Fluid .....	12
5	Phase Boundary in the $\rho, T$ plane. The path of integration in (33) is shown by the Dotted Line .....	23
6	The Main Part of the Apparatus .....	56
7	Gas-handling System .....	58

## I. INTRODUCTION

The critical phenomenon was discovered in 1822 by de la Tour.<sup>1</sup> In 1869 Andrews measured the critical temperature of CO<sub>2</sub>. His investigations<sup>2,3,4,5</sup> led to the concept that each gas has a lowest temperature above which it cannot be liquified no matter what pressure is exerted. This is the critical temperature.

The phase equilibrium curve in the T, P-plane terminates at the critical point, as shown in Fig. 1. The temperature of this point is the critical temperature  $T_C$ , while the pressure is the critical pressure. Of the most recent values for the critical temperature and the critical pressure of He<sup>4</sup> and He<sup>3</sup> are:

For He<sup>4</sup>:  $T_C = 5.1894^\circ\text{K}$  as reported by Edwards<sup>6</sup>

or  $T_C = 5.191 \pm 0.002^\circ\text{K}$  as reported by Roach and Douglass<sup>7</sup>.

While  $P_C = 170.8 \pm 0.3$  cm Hg (from Roach and Douglass<sup>7</sup>).

For He<sup>3</sup>:  $T_C = 3.3095^\circ\text{K}$  (Zimmerman and Chase<sup>8</sup>)

or  $T_C = 3.316^\circ\text{K}$  (Elwell and Meyer<sup>9</sup>)

or  $T_C = 3.3436^\circ\text{K}$  (Kerr and Sherman<sup>10</sup>)

$P_C = 86.75$  cm Hg (Elwell and Meyer<sup>9</sup>)

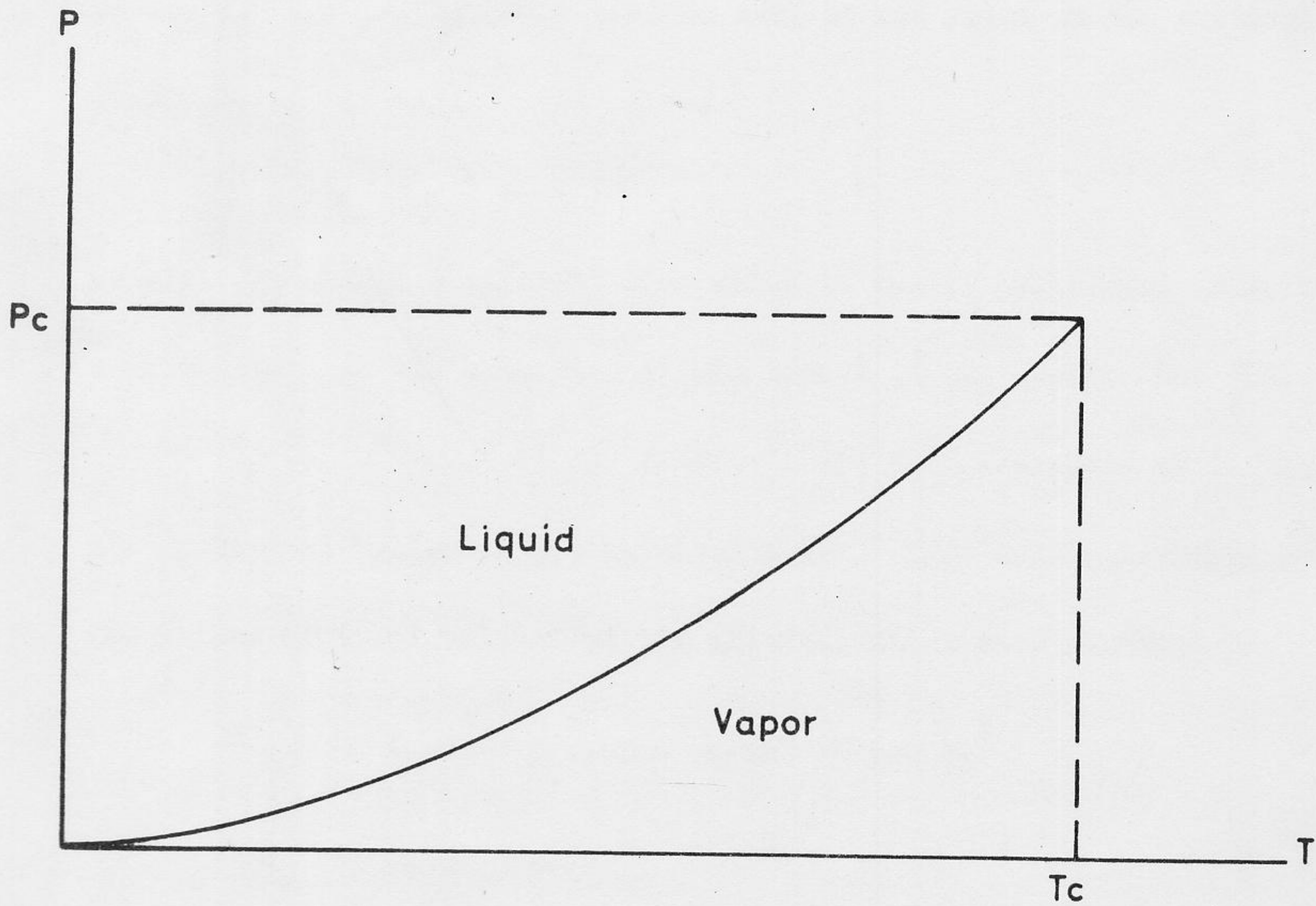
or  $P_C = 88.88$  cm Hg (Kerr and Sherman<sup>10</sup>)



The critical phenomenon was discovered in 1932 by de la Tour.  
In 1934 Andrews measured the critical temperature of CO<sub>2</sub>. His inves-  
tigations showed that the isotherms that occur are not a normal isotherm  
but have a point of inflection at the critical temperature and pressure.  
The phase equilibrium curve is the T-P curve in the T-P diagram of the  
critical point, as shown in Fig. 1. The temperature of this point is the  
critical temperature, T<sub>c</sub>, while the pressure is the critical pressure, P<sub>c</sub>.  
The real isotherms below the critical temperature are the normal  
isotherms of the gas.

Fig. 1.--The phase equilibrium curve

Fig. 1.--The phase equilibrium curve



An interesting feature of the liquid-vapor phase equilibrium appears if we draw the graph of the densities of the liquid under its saturated vapor pressure and of the saturated vapor versus the temperature. The two branches tend to meet at one point at the critical temperature. If we draw the curve:

$$\frac{1}{2}(\rho_l + \rho_g) \longleftrightarrow T$$

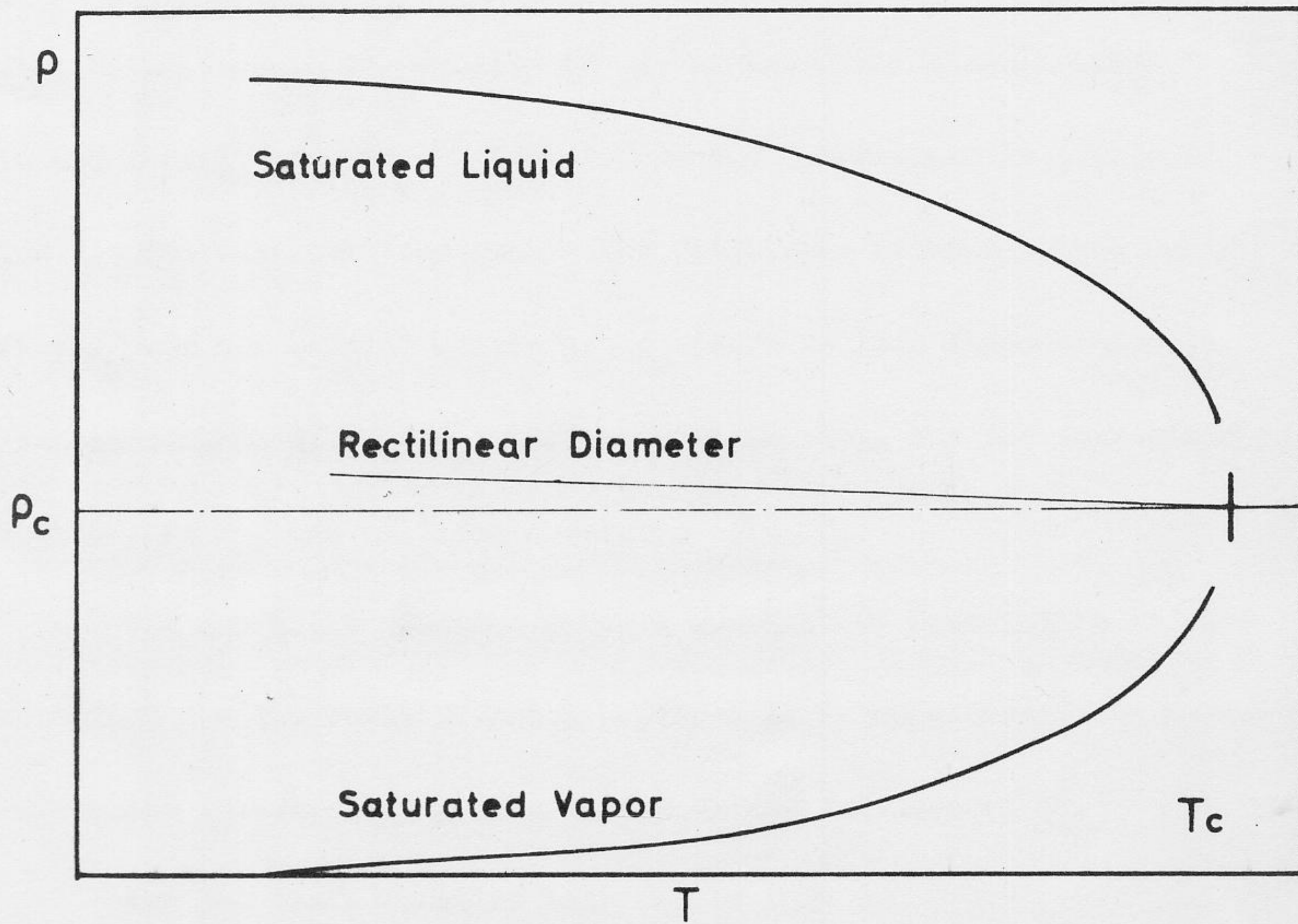
we will get almost a straight line which is nearly horizontal, slanting a little towards the saturated liquid branch of the graph. See Fig. 2.

The two branches of the density curve were extrapolated to find the density of helium at the critical point. From such extrapolations the values of the densities at the critical point were found to be:

$$\rho_C = 0.06948 \pm 0.0030 \text{ gm/cm}^3 \text{ }^{11} \text{ for He}^4$$

$$\rho_C = 0.04134 \text{ gm/cm}^3 \text{ }^8 \text{ for He}^3.$$

Fig. 2.--The densities of saturated liquid and saturated vapor, showing the rectilinear diameter.



## II. THEORY

At temperatures below the critical temperature a gas can be liquified by isothermal compression. Above this temperature the transfer from the dense gas to the liquid takes place without any discontinuities in the density or any higher order singularities in the density or other variables. As the temperature is increased towards the critical temperature the difference between liquid density  $\rho_l$  and the density of the gas  $\rho_g$  tends to zero ~~dis~~continuously. The limiting density is  $\rho_c$ , the critical density, and the corresponding pressure is  $P_c$ , the critical pressure. Fig. 3.

Van der Waals equation gives a qualitative description of condensation and the critical point provided it is supplemented by Maxwell's rule which ensures that  $\rho$  is a single valued function of  $P$ .

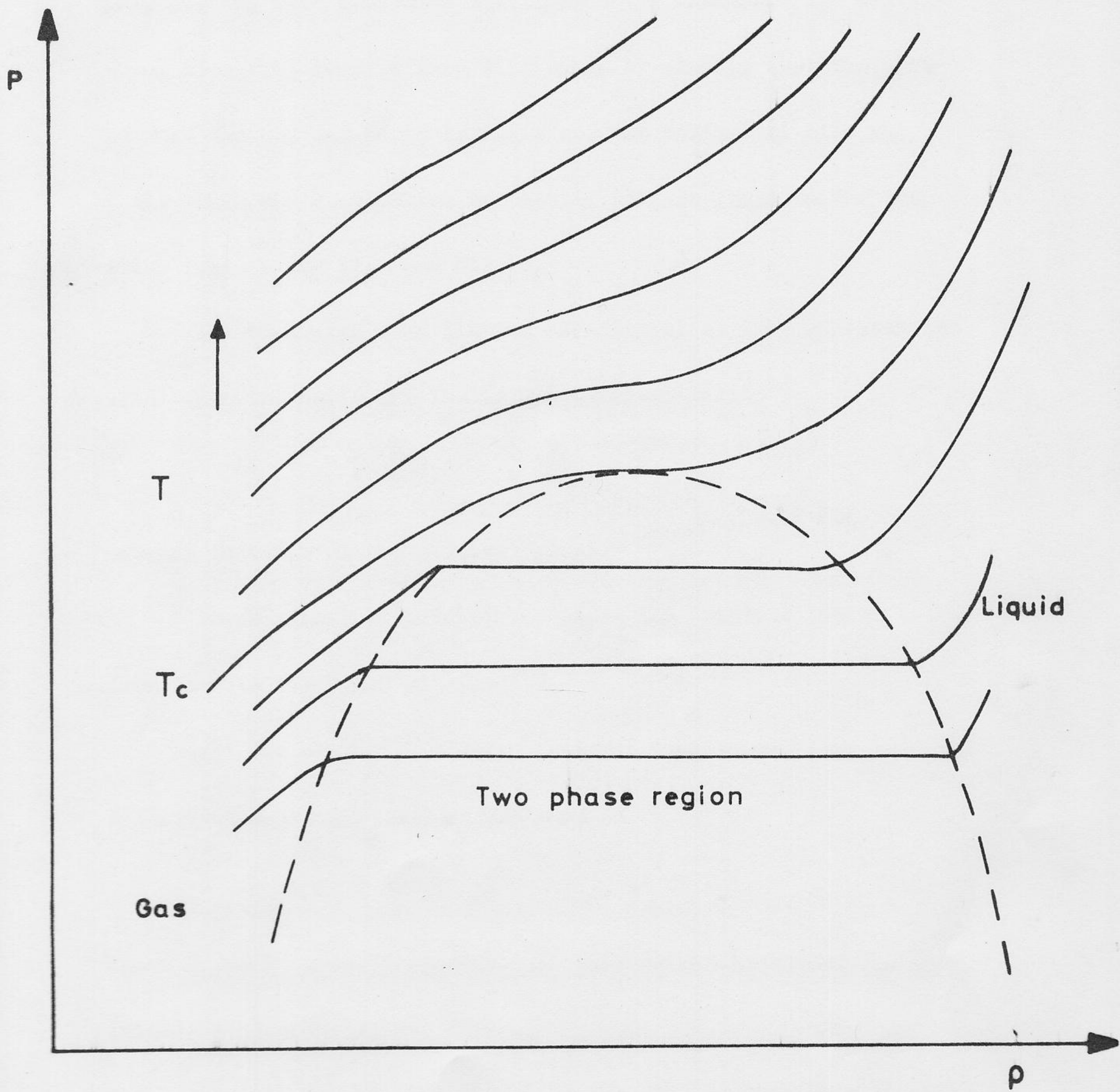
Van der Waals equation is:

$$\frac{P}{kT} = \frac{\rho}{(1-b\rho)} - \frac{a\rho^2}{kT} \quad (1)$$

The van der Waals isotherms of  $P$  versus  $\rho$  look similar to those of a real gas which are drawn schematically in Fig. 3 except for the horizontal lines corresponding to the two phase region for an equilibrium transition

Fig. 3.--Schematic isotherms for a simple fluid in the critical region.





of a real fluid. The van der Waals isotherms are continuous in this region, each including a maximum and a minimum. The Maxwell equal area rule removes this difficulty by stating that the area between the van der Waals isotherm and the horizontal line which falls above the equilibrium horizontal line is equal to the area which falls under it. See Fig. 4.

The isotherms grow flatter and flatter as they approach the critical point while the isothermal compressibility

$$K_T = -\frac{1}{V} \left( \frac{\partial V}{\partial P} \right)_T = \frac{1}{\rho} \left( \frac{\partial \rho}{\partial P} \right)_T \quad (2)$$

becomes infinite at the critical point.

Three principal predictions about the critical region follow from the van der Waals equation:<sup>12</sup>

a) The coexistence curve follow a square-root law, i.e. the difference between  $\rho_l$  and  $\rho_g$  vanishes as

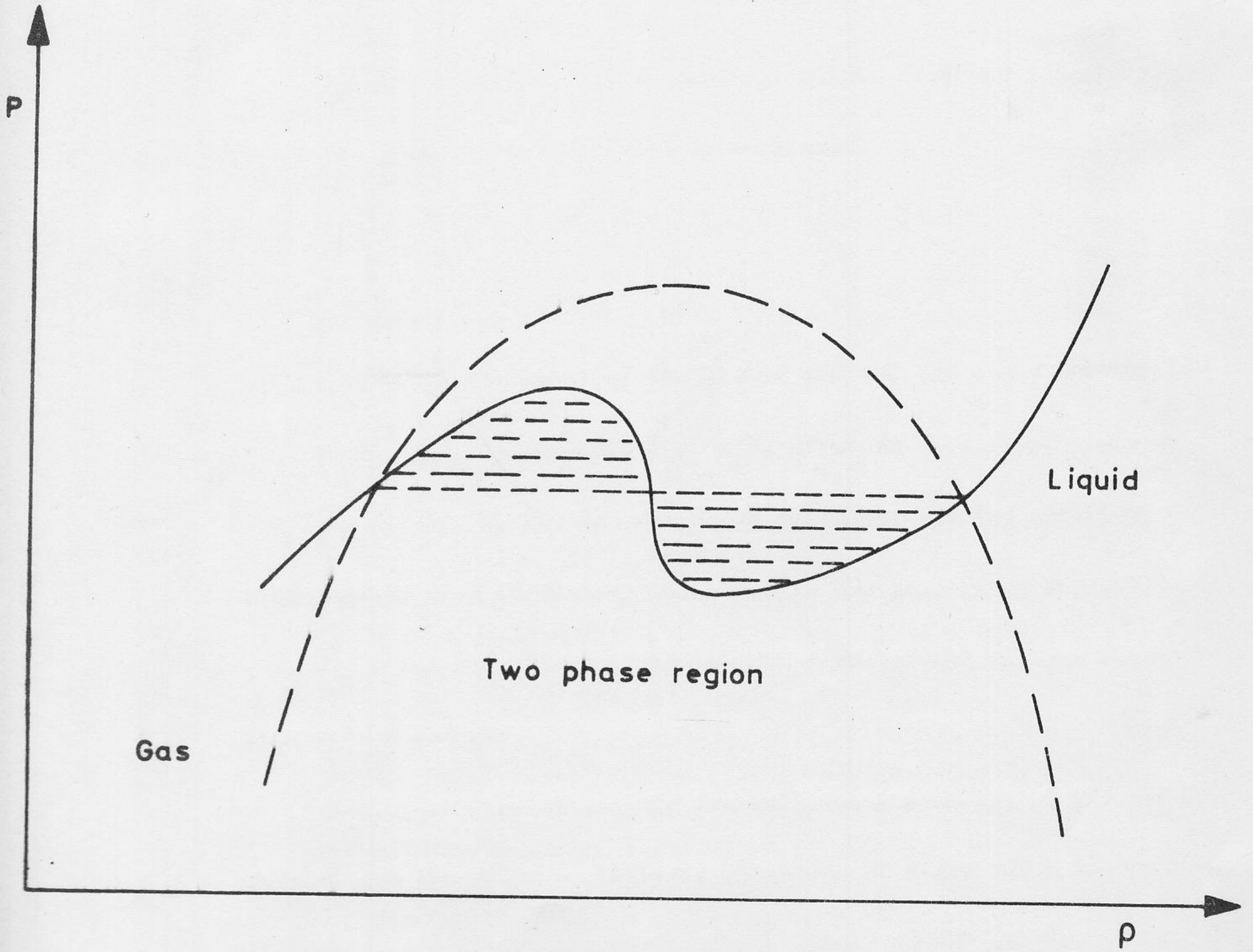
$$\rho_l - \rho_g \cong A(T - T_C)^{\frac{1}{2}} \quad (T \rightarrow T_C^-) \quad (3)$$

Where  $T \rightarrow T_C^-$  means approaching  $T_C$  from values less than  $T_C$ .

(Since for  $T > T_C$ ,  $\rho_l - \rho_g = 0$ ).

b) The compressibility along the critical isochore diverges

Fig. 4.--Schematic isotherm for a van der Waals fluid



as a simple pole

$$K_T \cong \frac{B}{(T-T_C)} \quad (T \rightarrow T_C^+, \rho = \rho_C) \quad (4)$$

c) The specific heat at constant volume rises to a maximum at the critical point then falls discontinuously:

$$C_V(T) \cong C_C^+ - D^+ |T - T_C| \quad T \gtrsim T_C \quad (5)$$

with  $C_C^- - C_C^+ = \Delta C > 0$ .

The compressibility of the liquid and the gas along the coexistence curve, i.e. at condensation, also diverges as a simple pole as  $T \rightarrow T_C^-$  according to the van der Waals equation, but the amplitude corresponding to B is smaller than that in equation (4). The constants A, B,  $C_C^+$ ,  $D^+$  can be written explicitly in terms of the van der Waals parameters a and b.

The above predictions are not only reached at by the van der Waals equation but all other approximate equations of state reach to the same conclusions. (See for example Landau's theory of the critical point and second order phase transitions, ref. 17). Indeed they are essentially a consequence of the implicit or explicit assumption that the free energy and the pressure can be expanded in a Taylor series near the critical

point. That is the free energy is not a singular point when expressed as a function of  $\rho$  and  $T$  (provided Maxwell's rule is applied for  $T < T_C$ ).<sup>12</sup>

The predictions of the classical theories can be tested by the data on the coexistence curves of simple gases. Guggenheim<sup>13</sup> showed that the gases Ne, Ar, Kr, Xe, N<sub>2</sub> and O<sub>2</sub> obey closely a law of corresponding states of the form:

$$(\rho_l - \rho_g) / 2\rho_c = A(1 - T/T_C)^\beta, \quad T \rightarrow T_C \quad (6)$$

with  $\beta = \frac{1}{3}$ . In earlier work on CO<sub>2</sub>, Michels, Blaisse, and Michels found that the coexistence curve near the critical point could be fitted by (6) with the index  $\beta = 0.357$ . In a very careful study of xenon, Weinberger and Schneider<sup>14</sup> obtained data which obey accurately the relation (6) with a nonclassical value of the index  $\beta$  near the critical point. Analysis of their measurements indicates that

$\beta = 0.345 \pm 0.015$  which is not inconsistent with a value of exactly  $\frac{1}{3}$ .

While it is possible that measurements taken much closer, than has been done, to the critical point may still yield the classical value  $\frac{1}{2}$

The accurate experimental measurement of the isothermal compressibility of a gas near its critical point is not easy. The experimental results, (e.g. those of H.W. Habgood and W.G. Schneider<sup>16</sup>), however, indicate  $K_T$  diverges more sharply than a simple pole, i.e.

$$K_T(T) \approx \frac{B}{|(T/T_C) - 1|^\gamma} \quad (\rho = \rho_C, T \rightarrow T_C) \quad (8)$$

with  $\gamma$  greater than 1.1.

One of the theories based on Taylor series expansions is the Landau-Lifshitz theory of the critical point.<sup>17</sup> Their assumptions are that the conditions

$$\left(\frac{\partial P}{\partial V}\right)_T = 0 \quad (9)$$

$$\left(\frac{\partial^2 P}{\partial V^2}\right)_T = 0 \quad (10)$$

and

$$\left(\frac{\partial^3 P}{\partial V^3}\right)_T < 0 \quad (11)$$

hold at the critical point, where  $V$  is the molar volume. Introducing the notation  $t = T - T_C$ ,  $v = V - V_C$ , they expand  $(\partial P/\partial V)_T$  as:

$$-\left(\frac{\partial P}{\partial V}\right)_T = At + Bv^2 \quad (12)$$

for small values of  $t$  and  $v$ .

Equation (12) may be integrated to give, for the equation of any isotherm

$$P = -Atv - \frac{1}{3}Bv^3 + f(t) \quad (13)$$

To solve for the values of  $v_g$  and  $v_l$  of saturated vapor and saturated liquid in equilibrium, they use the two conditions

$$\mu_l = \mu_g, \quad (14)$$

where  $\mu$  is the chemical potential, and

$$P_l = P_g. \quad (15)$$

Equation (14) is used in the form:

$$\int_l^g d\mu = \int_l^g v(\partial P/\partial v)_t dv = 0 \quad (16)$$

where  $\int_l^g$  means the integral along the transition curve from a state with one phase to a state with the other phase. Evaluating equation (16) using equation (12) gives

$$\frac{1}{2}At (v_g^2 - v_l^2) + \frac{1}{4}B(v_g^4 - v_l^4) = 0 \quad (17)$$

Equation (15) combined with equation (13) gives

$$At (v_g - v_l) + \frac{1}{3}B (v_g^3 - v_l^3) = 0 \quad (18)$$

Simultaneous solution of Equations (17) and (18) gives

$$v_g + v_l = 0 \quad (19)$$



$$v_L = - (-3At/B)^{\frac{1}{2}} \text{ or } v_L^2 = -3At/B \quad (20)$$

and

$$v_g = +(-3At/B)^{\frac{1}{2}} \text{ or } v_g^2 = -3At/B \quad (21)$$

Thus, Landau and Lifshitz predict that along the coexistence curve, at temperatures  $T_C$ ,  $v_g$  and  $v_L$  should be equal and opposite, and that  $v_L^2$  and  $v_g^2$  should be equal and proportional to  $-t = T_C - T$ .

Analysis of the experimental measurements of Edwards and Woodbury<sup>11</sup> show that the predictions of Landau and Lifshitz are in fault. Neither for the vapor nor for the liquid is the curve of  $v^2$  versus  $(-t)$  a straight line. The graph of  $v_g + v_L$  against  $-t$  should be a horizontal line through the origin if the equation  $v_g + v_L = 0$  were true. The experimental results are a clear contradiction of the Landau-Lifshitz prediction on this point.

In order to overcome the difficulties met by the Landau-Lifshitz theory when tested by experimental measurements, Edwards and Woodbury<sup>11</sup> modified the Landau-Lifshitz theory. Thus expanded

$$-\left(\frac{\partial P}{\partial V}\right)_T = At + Bv^2 + Ctv + Dt^2 \quad (22)$$

and stopped after reaching the second powers in  $t$  and  $v$ . Following the same procedure as that of Landau and Lifshitz they get the results:

$$v_g + v_L = -\frac{C}{B}t \quad (23)$$

$$v_L = -\frac{Ct}{2B} - \left[ 3t^2 \left( \frac{C^2}{4B^2} - \frac{D}{B} \right) - \frac{3At}{B} \right]^{\frac{1}{2}} \quad (24)$$

and

$$\frac{\left( v_g + \frac{Ct}{2B} \right)^2}{-3t} = - \left( \frac{C^2}{4B^2} - \frac{D}{B} \right) t + \frac{A}{B} \quad (25)$$

Analysis of the results of Edwards and Woodbury<sup>11</sup> shows good agreement between the equation for  $v_g + v_L$  and the experimental points up to 110 mdeg. from  $T_C$ . As regarding the volume-temperature curves better agreement than was reached at with the Landau and Lifshitz theory. But this expression leads to inconsistencies when applied at points away from the coexistence curve.<sup>18</sup>

Tisza and Chase<sup>19</sup>, to overcome these difficulties, at least partially, suggested interchanging the role of the variables  $N$  and  $V$ , ( $N$ : number of particles). Instead of considering a closed system with  $N$  fixed and  $v = \frac{V}{N}$  variable, as was done in the Landau-Lifshitz theory and its modifications by Edwards and Woodbury, they consider an open system with  $V$  fixed and  $\rho = \frac{N}{V}$  variable.

The analog of equation (12) is then:

$$V^{-1} \left( \partial^2 F / \partial \rho^2 \right)_{T,V} = \left( \frac{\partial \mu}{\partial \rho} \right)_T = \alpha T + \beta \rho^2 + \dots \quad (26)$$

By a treatment exactly parallel to that of Landau and Lifshitz in reference 17, they find,

$$\rho_l^* = \rho_l - \rho_C = -\rho_g^* = -(3\alpha t/\beta)^{\frac{1}{2}} \quad (27)$$

This expression fits as well with the Edwards and Woodbury results as their four-parameter expression.

Mistura and Sette<sup>20</sup> extended Tisza's expansion so as to include second order terms. They write

$$\frac{1}{V} \left( \frac{\partial^2 F}{\partial \rho^2} \right)_{T,V} = \left( \frac{\partial u}{\partial \rho} \right)_T = \alpha t + \beta \rho^{*2} + \gamma t \rho^* + \delta t^2 \quad (28)$$

and by development exactly analogous to that of Landau and Lifshitz in reference 17, they obtain,

$$\rho^* = -\frac{\gamma}{2\beta} t \pm \left[ 3t^2 \left( \frac{\gamma^2}{4\beta^2} - \frac{\delta}{\beta} \right) - \frac{3\alpha}{\beta} t \right]^{\frac{1}{2}} \quad (29)$$

where the negative sign is for the vapor and the positive for the liquid. According to this law the coexistence curve must be symmetric about a rectilinear diameter whose equation is

$$\frac{1}{2}(\rho_l + \rho_g) = \rho_C - (\gamma/2\beta)t \quad (30)$$

Considering these results, better agreement with the experiment is reached at than when the two terms expansion of Tisza was used.

Griffiths, however, pointed out<sup>21</sup> that if such an expansion as that of Mistura and Sette exists, it in itself and of itself precludes the possibility of any infinite singularity in  $C_V$ , at the critical point. His argument is as follows:

If one differentiates with respect to temperature the equation

$$\left(\frac{\partial \mu}{\partial T}\right)_\rho = - \left[ \partial \frac{(\rho S)}{\partial \rho} \right]_T \quad (31)$$

(where  $S$  is the molar entropy), the result,

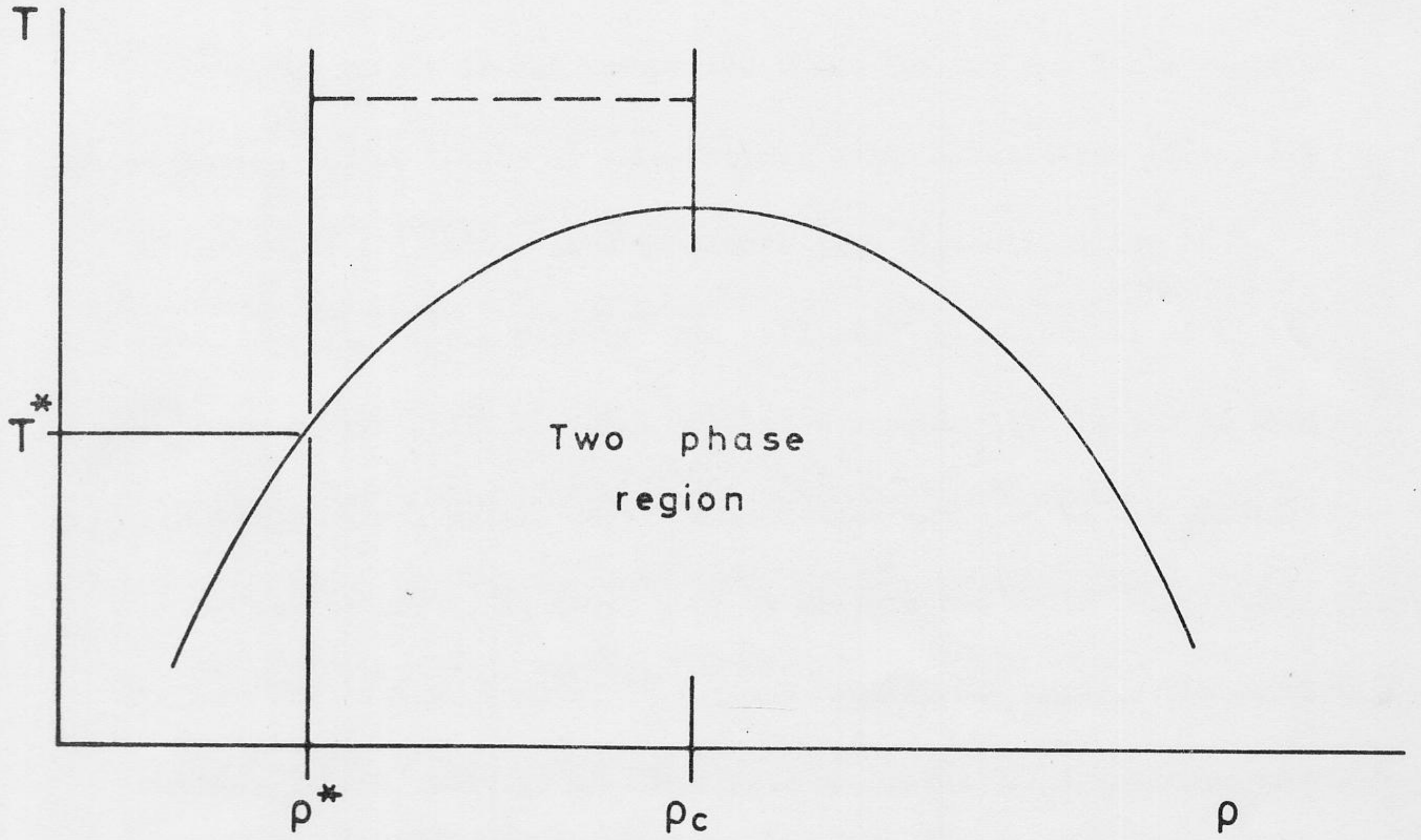
$$-T \left(\frac{\partial^2 \mu}{\partial T^2}\right)_\rho = \left[ \partial \frac{(\rho C_V)}{\partial \rho} \right]_T \quad (32)$$

may be integrated along the line of constant temperature  $T > T_C$  as shown in Fig. 4 to obtain

$$\begin{aligned} \rho_C C_V(\rho_C, T) - \rho^* C_V(\rho^*, T) &= -T \int_{\rho^*}^{\rho_C} \left(\frac{\partial^2 \mu}{\partial T^2}\right)_\rho d\rho \\ &= T(\rho^* - \rho_C) \left(\frac{\partial^2 \mu}{\partial T^2}\right)_{\rho=\rho_C} - T \int_{\rho^*}^{\rho_C} (\rho_C - \rho) \left(\frac{\partial^3 \mu}{\partial T^2 \partial \rho}\right)_{\rho=\rho^*} d\rho \end{aligned} \quad (33)$$

where  $\rho^*$  is a density near to but not equal to  $\rho_C$ . Since  $C_V(\rho^*, T)$  and  $\left(\frac{\partial^2 \mu}{\partial T^2}\right)_\rho$  are smooth (presumably analytic) functions of temperature for  $T > T^*$ , the temperature at which the  $\rho^*$  isochore intersect the phase boundary, one concludes, in particular, that they are finite and bounded

Fig. 5.--Phase boundary in the  $\rho, T$  plane. The path of integration in (33) is shown by the dotted line.



for temperatures above and including  $T_C$ . Thus if  $C_V$  is to diverge to infinity as  $T$  approaches  $T_C$  above the critical isochore, both integrands in (33) must diverge in contrast with (28) which implies that  $(\frac{\partial^3 \mu}{\partial T^2 \partial p})$  approaches the constant value  $\delta$ .

This result is not unexpected since the van der Waals equation of state, Landau theory of second-order phase transitions (Chap. XIV of reference 17), etc., lead to simple jump discontinuities in the specific heat. Since Moldover and Little's<sup>22</sup> measurements of  $C_V$  in  $He^4$  near to the critical point suggest a singularity similar to that observed at the  $\lambda$  point, there remains some doubt as to the significance of the parameters  $\alpha$ ,  $\beta$ , etc., used by Mistura and Sette<sup>20</sup> in fitting the data of Edwards and Woodbury<sup>11</sup> for the coexistence curve. The original<sup>11</sup>, and more recent analysis of these data suggest a coexistence curve which is parabolic<sup>19,23</sup> or almost parabolic<sup>24</sup> at the top. This result is not directly related to whether there is or there is not an infinite singularity of  $C_V$  at the critical point. Equation (28), however, includes more information than the shape of the coexistence curve, and this is why its validity is questioned.

Griffiths proof breaks down if the expansion in (28) is terminated after the second term, as was done by Tisza and Chase<sup>19</sup>, since then the required singularities in (33) could be provided by the second temperature derivative in the remainder term. However, it is not even safe to assume the expansion can be carried out this far. Griffiths<sup>21</sup> illustrates with a simple example taken from the class of "homogeneous functions" discussed by Widom.<sup>25</sup>

$$\mu = \mu_0(T) + \{at\rho' + b\rho'^3 + c\rho'^3 \operatorname{Re} [id + t^2 \rho'^{-4}]^{\frac{1}{2}}\} \quad (34)$$

where  $\mu_0(T)$  is the chemical potential along the critical isochore;  $\operatorname{Re}$  means the real part;  $i = \sqrt{-1}$ ;  $a$ ,  $b$ ,  $c$ , and  $d$  are positive constants. The coexistence curve, defined by vanishing of the expression in the curly brackets, is parabolic and  $C_V$  as a function of  $T$  along the critical isochore has a logarithmic singularity plus a superimposed discontinuity at the critical point.<sup>25</sup> It may be verified that no expansion of the form (28) terminating after the first two terms is valid for (34).



Thus, in conclusion, if, as is now believed, singularities occur at the critical point, the whole expansion procedure is questionable, since the coexistence curve cannot, in principle, be represented asymptotically by a Taylor series in the density about such a nonanalytic point.

Buckingham<sup>26</sup> discussed the nature of the singularity to be expected at the critical point of a system which could be said to have a "classical" critical point in what he called the "zeroth order" approximation. He showed that the specific heat diverges logarithmically. He obtained a first order approximation of which the preliminary results lead to a coexistence curve different from the classical one, which is a quadratic relationship between the density difference between the two phases and the temperature difference from the critical temperature. The coexistence curve resulting from Buckingham's theoretical derivation is:

$$\Delta\rho = \rho_l - \rho_g \propto (-t - \ln t)^{\frac{1}{2}} \quad (35)$$

or, equivalently,

$$\frac{(\Delta\rho)^2}{-\ln\Delta\rho} \propto t \quad (36)$$

Buckingham<sup>26</sup> suggested the use of the natural variable  $x = (\rho_L - \rho_g)/(\rho_L + \rho_g)$ . Edwards<sup>24</sup> pointed out the usefulness of this variable:

(1)  $x$  ranges from 1 to 0 as  $T$  ranges from zero to  $T_C$  for any substance.

(2) There is equal symmetry using either the density or the molar volume, since  $x = \frac{\rho_L - \rho_g}{\rho_L + \rho_g} = \frac{V_g - V_L}{V_g + V_L}$ .

(3) While for the customary use of the quantity  $\rho_L - \rho_g$ , or  $(\rho_L - \rho_g)/2\rho_C$  as a function of  $(T_C - T)$ , the slope of the "rectilinear diameter," differs from substance to substance, so that the similarity of the coexistence curves may be obscured by comparing experimental data in that matter, the use of  $x$  removes entirely this effect of the "rectilinear diameter."

(4) We can plot  $x^n$  against  $T$  without previous knowledge of  $T_C$  or  $\rho_C$  or  $V_C$ . In fact  $T_C$  may be determined by such plots.

Using this variable the expression for the asymptotic coexistence curve is<sup>26</sup>

$$\frac{x^2}{-\ln x} \text{ ct.} \quad (37)$$

But this is not suitable for comparison with experiment because of the spurious jump at  $x = 1$ . An expression with the same asymptotic form, but with the correct limit at  $T = 0$  is,

$$\frac{x^2}{1 - \ln x} \propto t.$$

This expression (in which the coefficient unity multiplying  $\ln x$  is arbitrary) has been compared by Edwards<sup>24</sup> with his measurements for the coexistence curve. He also compared his measurements with the analytic relations,

$$x^2 \propto t \tag{38}$$

and  $x^3 \propto t$  (39)

He found that the nonanalytic relation

$$\frac{x^2}{1 - \ln x} \propto t, \tag{40}$$

is the best asymptotic form, fitting well above  $0.96 T_C$ .

The Critical Exponents and Quantum Deviations

A. Theory

The critical exponents  $\alpha$ ,  $\beta$ ,  $\gamma$  have been defined above.

The exponent  $\delta$  is defined in the following relation:

$$|P - P_C| \sim |\rho - \rho_C|^\delta \quad T = T_C \quad (41)$$

Some experimental evidence (see section B, p. 32) tends to indicate that the critical exponents characterizing the liquid-gas phase transition are markedly different for the light substances He, H<sub>2</sub> and D<sub>2</sub>, when compared with the results for the heavier elements Xe, Kr, Ar, N<sub>2</sub>, O<sub>2</sub> and Ne. In particular, while the coexistence curves of Xe and CO<sub>2</sub> may be described accurately over a wide range of T approaching T<sub>C</sub> by

$$(\rho_L - \rho_g)/2\rho_C \approx D(1 - T/T_C)^\beta$$

with  $\beta$  lying in the range 0.33 to 0.36<sup>12,14,41,42</sup>; the apparent value of  $\beta$  (e.g. on a log-log plot) for He<sup>3</sup> and He<sup>4</sup> seems to increase to values in the range 0.40 - 0.50 when  $T/T_C \geq 0.98$ <sup>24, 27</sup>. Similar changes towards "van der Waals - like" behavior appear to take place also in the other critical-point exponents ( $\gamma$  and  $\gamma'$  for the compressibility above and below T<sub>C</sub>, etc.).<sup>12,28,29</sup> If we assume for the moment that the experi-

ments are correct in indicating this difference then we must look for a parameter which measures quantum behavior. It is quite reasonable to assume that the different behavior of the light elements is due to the quantum-mechanical dispersion<sup>30</sup> in the position of the molecules, which occurs when the kinetic energy of the molecule is comparable to its effective potential energy. To give this statement some quantitative substance a discussion of the law of corresponding states is helpful. Considering first the classical problem, as formulated by de Boer.<sup>31</sup>

Assume the interaction between the molecules was given by the potential energy  $\varphi(r)$ . We can apply a law of corresponding states if for different fluids

$$\varphi(r) = \Delta f(r/\sigma) \quad (42)$$

where  $f(r/\sigma)$  has the same form for all fluids, that are not necessarily only monoatomic, but behave as molecules with a spherical potential field

$\varphi(r)$ , given above, as for instance hydrogen, deuterium and nitrogen.

For such fluids, however, the additional assumption that the vibration and rotation of the molecules are not influenced by the position of the neighbouring molecules, should be made. Then  $\Delta$  and  $\sigma$  are the characteristic

energy and length for the fluid in question. We may compare different fluids by using the reduced variables:

$$T^* = kT/\Delta, \quad V^* = V/N\sigma^3, \quad P^* = P\sigma^3/\Delta \quad (43)$$

Since the potential energy function (42) determines all of the statistical properties of a classical fluid,  $P^*$  should be the very same function of  $V^*$  and  $T^*$  for different fluids as long as quantum corrections are unimportant. The values of the critical reduced pressure, temperature and specific volume are found to be nearly the same for the heavier fluids.<sup>32</sup>

The kinetic energy, however, is important in quantum statistical mechanics. If a particle is localized in a volume of order  $\sigma^3$ , it has a kinetic energy of the order

$$h^2/m\sigma^2 \quad (44)$$

according to the uncertainty principle. The size of the quantum correction can be estimated by comparing (44) with the typical potential energy  $\Delta$ . The ratio of these two energies:

$$(\Lambda^*)^2 = h^2/m\sigma^2\Delta \quad (45)$$

is a dimensionless measure of the importance of quantum effects in

the liquid-gas transition. As  $\Lambda^*$  becomes larger than unity (in  $H_2$ ,  $He^4$  and  $He^3$ ) the critical reduced pressure, temperature and volume deviate from their classical values.<sup>32</sup>

### B. Experiment

Moldover and Little<sup>22</sup> measured the specific heats of  $He^3$  and  $He^4$ . Kadanoff et al<sup>32</sup> fitted the results of Moldover and Little to the formula

$$\begin{aligned} C &= a e^{-\alpha} + b && \text{for } T > T_C && (46) \\ &= a' (-\epsilon)^{-\alpha'} + b' && \text{for } T < T_C \end{aligned}$$

where  $\epsilon = (T - T_C)/T_C$  (47)

and  $a$ ,  $a'$ ,  $b$  and  $b'$  are adjustable parameters.  $\alpha'$  then lies between 0.0 (logarithmic singularity) and 0.2 and  $\alpha$  between 0.0 and 0.3.<sup>32</sup>

This conclusion, however does not include a possible perturbation due to gravitational effects. According to a calculation based on the Landau theory<sup>33</sup>, using the data of Edwards and Woodbury<sup>11</sup>, a 1% density variation might exist in this experiment for  $\epsilon < 5 \times 10^{-4}$ . This could cause a rounding of the specific heat peak.

The critical exponent  $\beta$  was measured by Edwards and Woodbury<sup>11</sup> for He<sup>4</sup> by using a Jamin interferometer. They measured the index of refraction of a "slice" of Helium 1 mm thick and from this determined the density using the Lorentz-Lorenz equation. The correction to this equation near the critical point has been estimated to be negligible using a theory of Larsen, Mountain and Zwanzig<sup>\* 34</sup>. The results of this experiment have been fitted to many analytical expressions.<sup>11,19,20,24</sup> Unfortunately, this experiment does not permit an unambiguous conclusion about  $\beta$ . By varying  $T_C$  the assumed range for the critical region within reasonable limits, it is possible to have  $\beta$  between 0.40 and 0.50.<sup>32</sup>

The results of recent measurements by Roach and Douglass<sup>35</sup> are that  $\beta = 0.35 \pm 0.01$  for  $4 \times 10^{-4} < (-\epsilon) < 2 \times 10^{-2}$ . They measured the dielectric constant of helium between two plates and obtained the density using the Clausius-Mosotti equation. Edwards<sup>6</sup> has repeated his measurements,

---

\* They evaluated corrections to the Lorentz-Lorenz equation, due to long-range density fluctuations, using Yvon's statistical-mechanical theory of the refractive index, together with the Ornstein-Zernike asymptotic form of the two-particle correlation function. For argon, with experimentally reasonable values for the numerical parameters, the correction is smaller than one part in  $10^4$ .



and his most recent result is that  $\beta = 0.37 \pm 0.02$  for  $2 \times 10^{-4} < (-\epsilon) < 10^{-2}$ .

Thus it appears that  $\beta$  is about the same for  $\text{He}^4$  as in the classical gases.

The coexistence curve for  $\text{He}^3$  has been determined by Sherman<sup>27</sup> by measuring the pressure as a function of temperature using a constant volume bomb with 23 different densities. The pressure-temperature relations are nearly linear, and are extrapolated to the known vapor-pressure curve to obtain temperature-density data. This method has the advantage of giving the entire shape of the PVT surface in the critical region and not only  $\beta$ . Furthermore, the effect of gravity and the infinite compressibility is avoided since no part of the fluid is at the critical point. However, the extrapolation to the vapor-pressure curve is questionable, since it is not known definitely that the isochores (constant volume) continue to be linear in the immediate neighborhood of the critical point.<sup>32</sup>

Kadanoff et al.<sup>32</sup> fitted Sherman's<sup>27</sup> data for  $2.5 \times 10^{-2} < (-\epsilon) < 2.5 \times 10^{-1}$  with  $\beta = 0.36 \pm 0.02$ . Since Sherman's published data<sup>27</sup> include only two data points for  $(-\epsilon) < 2.5 \times 10^{-2}$ , Kadanoff et al. did not feel justified in estimating  $\beta$  in this region. However the data suggest a possible increase in  $\beta$  towards 0.5.<sup>32</sup>

Fisher<sup>23</sup> proposed an explanation for the apparent dependence on  $\beta$  which was noted by Sherman. He suggested that the variation of  $\beta$  might reflect the behavior of a system in which quantum corrections are not very large. The value of  $\beta$  for large  $\epsilon$ , i.e. far from  $T_C$  will be then classical  $\beta \approx \frac{1}{3}$ , while near the critical point, the more delicate quantum effects are important and  $\beta$  changes its value to that characteristic of a quantum system.

This apparent dependence on  $\epsilon$  of  $\beta$  seems questionable in view of the results for  $\text{He}^4$  obtained by Roach and Douglass.<sup>35</sup> They found that  $\beta$  is independent of  $\Lambda^*$ , the quantum correction parameter, over the range  $0.06 < \Lambda^* < 2.6$  (Xe to  $\text{He}^4$ ), so that  $\beta$  would have to change very rapidly over the range  $2.6 < \Lambda^* < 3.1$  ( $\text{He}^4$  to  $\text{He}^3$ ) to explain the apparent<sup>27</sup>  $\beta \approx 0.48$  in  $\text{He}^3$ .

The coexistence curve for hydrogen has been determined by the isochoric method,<sup>36</sup> and the data can be fitted with  $\beta = 0.36 \pm 0.01$  for  $\epsilon > 10^{-2}$ . There is an indication that  $\beta$  becomes larger ( $\approx 0.50$ ) for  $\epsilon < 10^{-2}$ , but this might be due to the effect of gravity.

Considering now the exponent  $\gamma$  for the isothermal compressibility. From Sherman's<sup>27</sup> compressibility data  $\gamma = 1.09 \pm 0.05$ .

Below  $T_C$   $\gamma'$  is evaluated along the two branches of the coexistence curve. This yields two different  $\gamma'$  values:

$$\gamma'_g = 1.00 \pm 0.05 \text{ (gas)}$$

$$\gamma'_l = 1.18 \pm 0.10 \text{ (liquid)}$$

These values of  $\gamma$  are obtained from derivatives of PVT data, so they necessarily have large uncertainty. Also uncertain are the size of the critical region and the extrapolation procedure to the coexistence curve. In view of these difficulties one must conclude that a definite measurement of  $\gamma$  probably closer to the coexistence curve and for smaller values of  $\epsilon$ <sup>32</sup> is required.<sup>32</sup>

The shape of the critical isotherm is characterized by the exponent  $\delta$ . Sherman<sup>27</sup> interpolated his data to the critical isotherm to obtain the density as a function of pressure and found  $\delta = 3.4 \pm 0.2$ . Chase and Zimmerman<sup>28</sup> measured  $\delta$  more directly by measuring the dielectric constant of He<sup>3</sup> as a function of pressure at  $T = 3.324^{\circ}\text{K}$ . Then using the Clausius-Mosotti relation to find the density, they determined  $\delta = 3.5 \pm 0.1$ . Their

data indicate that the coefficient A in the equation

$$\left| (P - P_C)/P_C \right| = A \left| (\rho - \rho_C)/\rho_C \right|^\delta \quad (48)$$

is twice as great for the high-density fluid as for the low-density fluid. This difference between high and low density is also seen in Sherman's determination of  $\gamma_L$  and  $\gamma_g$ . The shape of the critical isotherm for  $H_2$  has been calculated from the data of Johnson, Keller and Friedman<sup>37</sup> by Widom and Rice<sup>38</sup>, who found  $\delta = 4.2$ . However, these data required a long extrapolation to find  $\delta$ <sup>29</sup>, which therefore may be unreliable.

In conclusion, there is no strong indication that the quantum fluids behave differently from the classical fluids in the critical region.

### III. EXPERIMENTAL

#### Difficulties Encountered in Measurements in the Critical Region

Measurements in the critical region are difficult to make.

This is true for all fluids, but it is especially difficult to perform experiments in the critical regions of fluids with very low critical temperatures like He<sup>3</sup> and He<sup>4</sup>.

One of the problems to be faced with in such measurements is that the system is usually very susceptible to minute amounts of impurities. A further complication arises from the large heat capacity of a fluid near critical conditions. Equilibrium times become very long near the critical point as a result of this, necessitating waits of perhaps days before it is reasonably certain that equilibrium conditions have been attained.<sup>32</sup> For example in the measurements of Bagatski, Voronel' and Gusak<sup>15</sup> of  $C_V$  for argon near the critical point, they had to wait 5 - 6 hours for each measurement to reach equilibrium, continuously stirring the liquid in the calorimeter. Failure to do this leads to nonreproducibility of the data. The time found necessary to attain equilibrium near  $T_C$  for measurements on  $C_V$  of Oxygen by Voronel' et al<sup>39</sup> was 3 - 4 hours if the liquid is

simultaneously mixed. Amirkhonov and Gurvich<sup>40</sup> measured the heat-capacity of water-phenol solutions through the critical region with and without stirring in the calorimeter. Careful temperature measurements in the calorimeter indicated the presence of large temperature gradients when no mixing occurred. It is suggested that the decreased heat transmission throughout the solution is a result of the experimentally observed increase of viscosity of solutions near the critical point which would result in a decreased intensity of convection.

Moreover, near the critical point one must contend with the extremely large compressibilities. Due to the weight of the fluid, only a very narrow range of vertical height achieves critical pressure at one time in a sample bomb (theoretically of course, only a single horizontal plane of the sample could be at critical pressure at one time). Therefore, in a PVT measurement what is measured is the average condition of the fluid. Unless special precautions are taken, this may be quite different from the critical condition, and can lead to a flat top in the coexistence curve<sup>41</sup>, (liquid-gas density difference as a function of temperature. One of the most elegant methods of dealing

with this was devised by Lorentzen<sup>41,42</sup>, who used a long vertical tube as this cell and measured the density of the fluid as a function of height near the critical region by the refraction of parallel light beams passing through the cell.

To obtain satisfactory results in such measurements, temperature control is critical. In some of the experiments involving the critical points in fluids, the data do not seem to settle down to its asymptotic critical behavior until  $\epsilon = (T - T_C)/T_C$  gets smaller than  $10^{-2}$ . A temperature control system must be able to maintain and reproduce temperatures to perhaps one part in  $10^4$  of  $T_C$  in order to provide meaningful data over a two decade range in  $\epsilon$  within this region. Since this control is most easily achieved near room temperature, the most complete data are available for the classical gases Xe ( $T_C = 289.6^\circ\text{K}$ ) and  $\text{CO}_2$  ( $T_C = 304.0^\circ\text{K}$ ).<sup>32</sup>

The difficulties encountered when dealing with helium, at the critical region, apart from the usual problems of gashandling at low temperatures, are due to the lack of a suitable cryogenic liquid that can be kept at the critical temperature of  $\text{He}^4$ .

So far, most of the research investigations at low temperatures made use of the dielectric constant<sup>8,9,35</sup> or the refractive index<sup>11</sup> of the helium isotopes. The densities are then obtained from the dielectric constant by means of the Clausius-Mossotti relation, or from the refractive index by means of the Lorentz-Lorenz equation. In both cases the polarizability is assumed to be constant. "To what extent is the polarizability dependent on density and temperature?" is a question which Kerr and Sherman<sup>10</sup> attempted to answer. They reported a deviation in the polarizability, of the order of 2% in compressing to the critical density. This ought to be accounted for when the experimental values of the dielectric constant or the refractive index are to be used to obtain density data.

The method suggested in this thesis for acquiring PVT data has the advantage of being a direct method. The volume measurements, made by a magnetic technique, require no use of equations which assume constant polarizability. Therefore, the problems of correcting for the deviation of the polarizability does not arise in this case. Thus, by making measurements with such an apparatus, the validity of the optical and dielectric methods can be checked.



### The Apparatus

An apparatus was constructed for PVT measurements in the critical regions of  $\text{He}^3$  and  $\text{He}^4$ . The sample is contained in a bellow (Fig. 6 - part 1), the pressure in which is to be measured with the help of a mercury manometer (see Fig. 7) connected to the bellow and a Texas Instruments fused bourdon tube gauge (Fig. 7 - part 14) connected to the space outside the bellow (Fig. 6 - part 3). The temperature is to be monitored by means of a germanium thermometer (Fig. 6 - part 7) glued to the cell which surrounds the bellow (Fig. 6 - part 4). The volume measurements are to be taken by observing the inductance of a coil (Fig. 6 - part 5) which changes with the position of a ferroxcube (Fig. 6 - part 2) inside it. The ferroxcube is glued to a disc soldered to the bottom of the bellow and thus changes its position according to the volume of the bellow. The necessary low temperatures are obtained by means of a liquid helium cryostat (Fig. 7 - part 10). Cooling of the sample is achieved with the help of a regulated flow of cold through a copper rod (Fig. 6 - part 18) from the liquid helium in the cryostat to the pot. A heater

(Fig. 6 - part 9), which is carefully designed, controls the cooling to the desired temperature. The heat flow from the top of the cryostat is eliminated by a vacuum shield (Fig. 6 - part 11 and 14), which is cooled in the same manner as for the pot. The main parts of the apparatus are discussed in more detail below.

1. The Bellow and the Cell that Surrounds it

The bellow is that part of the apparatus which contains the sample of fluid on which the PVT measurements are to be made. It is a flexible box of 12.5 mm length, 12.5 mm outside diameter, and 8 mm inside diameter. It is a Servometer Corporation electro-deposited type nickel bellow. Of its advantages is its retained toughness at very low temperatures, its negligible hysteresis, its absolute leak tightness and its ability to withstand a net pressure of two atmospheres. Fig. 6 illustrates the main part of the apparatus, which includes the bellow. The bellow is connected via a very narrow stainless steel capillary of inner

diameter 0.172 mm and outer diameter 0.35 mm, of length 33 cm, soldered to a copper capillary of inner diameter 0.600 mm. The purpose of using the copper capillary is the large heat conductivity of copper. By protecting the copper capillary from the cold gas stream with wool, it is kept at room temperature. The temperature of the lower end of the copper capillary can be checked. This allows us to make accurate corrections for dead space. The copper capillary is connected to the gas handling system which contains the mercury manometer and through which He gas is pumped into the bellow. To the free end of the bellow a brass disc with a little rod in its middle is soldered with soft solder. To this little rod a <sup>piece of</sup> ferroxcube is glued. The ferroxcube is of 4 mm outside diameter and 11 mm length. The ferroxcube is surrounded by a coil whose inductance can be measured by means of an AC Anderson bridge. The temperature dependence of the ferroxcube has to be accounted for by measuring the inductance of the coil as a function of temperature only,

repeating with different differential pressures over the bellow.

The coil is separated from the walls of the copper cell, to which the bellow is soldered by soft solder, by a teflon spacer. This helps to hold the coil firm in its position and to minimize the eddy currents which may form in the copper walls. The copper pot surrounding the bellow is to be filled with He<sup>4</sup> to provide the pressure required to keep the net pressure on the walls of the bellow less than two atmospheres. Increasing the pressure in this pot reduces the volume of the bellow, while the volume of the dead space remains constant. At the critical point, where the compressibility is infinite, the change in the volume of the bellow can still be observed, even though the pressure remains constant. The part of the copper pot which is on top of the bellow is a separate chamber to be filled with liquid hydrogen. This chamber is connected to a hydrogen reservoir via a stainless steel capillary. This capillary is enveloped in another capillary of a larger diameter and the space between them is evacuated. With the additional help of two copper radiation shields soldered to the outside capillary near to the top of the pot, the non-blocking of

this capillary is ensured. The blocking of the capillary due to the freezing of hydrogen could be a problem. The copper cell is surrounded by a copper vacuum jacket which serves as a radiation shield. Soft solder was used for soldering all the capillaries. Woods metal solder was used in soldering the liquid hydrogen pot to the pot which surrounds the bellow. Woods was also used for soldering the top of the vacuum jacket while its bottom was soldered with hard solder.

## 2. Germanium Thermometer

As is seen in Fig. 6, a germanium thermometer is glued to the side of the pot which surrounds the bellow. This is a Texas Instrument glass encapsulated model with two platinum leads, the shorter of which is glued to the body of the pot. The germanium thermometer is useful for its accurate, reliable and rapid measurement of temperature between  $1.0^{\circ}\text{K}$  and  $40^{\circ}\text{K}$  and for its good reproducibility. At liquid He temperatures, thermometer resistance is about 2 K ohms or more. At room temperature its resistance is about 10 ohms. The reproducibility of this kind of thermometer is better than  $\pm 0.05\%$  T.

The germanium thermometer is to be calibrated against the  $\text{He}^4$  vapour pressure between, say  $2^\circ\text{K}$  up till just below  $T_C$ , for example till  $5.1^\circ\text{K}$ . Then the thermometer is calibrated between  $14^\circ\text{K}$  and  $20^\circ\text{K}$  against the  $\text{H}_2$  vapor pressure. (The hydrogen is placed in the chamber above the bellow.) Interpolation is then used for calibration of the temperatures in between. The error due to interpolation will not exceed  $0.5 - 1 \text{ m}^\circ\text{K}$  per  $0.1^\circ\text{K}$  of interpolation.

The temperature is to be measured by measuring the resistance of the germanium thermometer connected to the cell, the temperature of which is assumed to be equal to that of the bellow. The resistance of the germanium thermometer is measured with the help of a Keathley 150 AR micro-volt ammeter and a D.C. bridge with very special resistance boxes. (Electro Scientific Industries, type DB62.).

### 3. Temperature Control System

In Fig. 6 two stainless steel discs (parts 17) are soldered to the bottoms of the vacuum jacket and a copper box with hard solder. The copper box is in good heat contact with the pot that surrounds the

bellow. The stainless steel discs are each of 2 cm diameter and 0.25 cm thickness.\* They are soldered to two copper rods (Fig. 6 - parts 18), in the case of the disc soldered to the bottom of the copper box with hard solder, while in the case of the other disc with soft solder. The copper rods are about 37 cm long and have 1 cm diameters. The copper rods are immersed in the liquid helium bath, and serve as heat dissipators. The rod which conducts heat from the pot that surrounds the bellow is soldered with soft solder to a thin-walled stainless steel cylinder (Fig. 6 - part 20) which is soldered at its other end to the vacuum jacket. This cylinder reduces the heat conduction from the vacuum jacket to the bellow surroundings. The cross-sections of the stainless steel discs and copper rods were chosen to be of value large enough so that the heat supply through the capillaries from the top of the cryostat is balanced by the heat dissipation in the liquid helium bath. Because of the large difference in the heat conductivity between copper and stainless steel at low temperatures, most of the temperature drop will be through the stainless steel discs. The copper rods will not have much difference

\* The stainless steel parts that were used in the already built apparatus are of 0.5 cm diameters and 2.4 cm length. More careful calculations show that these dimensions are not sufficient for heat dissipation. When the apparatus is to be used, these parts should be replaced by discs with the dimensions suggested in the text.

in the temperature from one end to the other. This eliminates the effect of the height of the liquid helium level in the rate of cooling, which otherwise might be affected by how much the rods are immersed in the liquid helium bath.

The calculation for the heat input and the heat dissipation is discussed below:

Using a log-log graph of the heat conductivity of stainless steel versus temperature, the heat conductivity of stainless steel was found to be:

$$\lambda_1 = 0.000617 T^{1.21} \quad \text{for } T \text{ in the range } 1 - 18^\circ\text{K}$$

$$\lambda_2 = 0.00263 T^{0.745} \quad \text{for } T \text{ in the range } 18 - 70^\circ\text{K}$$

$$\lambda_3 = 0.00485 T^{0.60} \quad \text{for } T \text{ in the range } 70 - 300^\circ\text{K}$$

The rate of heat transfer is given by the formula

$$\dot{Q} = \frac{A}{L} \int_{T_1}^{T_2} \lambda(T) dT$$

where  $\dot{Q}$  is the rate of heat transfer,  $A$  is the cross-sectional area,  $L$  is the length of the heat transferring element,  $\lambda$  is the heat conductivity and  $T$  is the temperature.



Applying this relation to the heat transfer through the largest capillary in the system, which is soldered to the vacuum jacket, and through which the significant portion of heat is transferred:

$$\begin{aligned} \dot{Q} &= \frac{A}{L} \left( \int_3^{18} 0.000617 T^{1.21} dT + \int_{18}^{70} 0.00263 T^{0.745} dT \right. \\ &\quad \left. + \int_{70}^{300} 0.00485 T^{0.60} dT \right) \\ &= \frac{A}{L} \left[ 0.000617 \left( \frac{1}{2.21} \right) T^{2.2} \right]_{3}^{18} + 0.00263 \left( \frac{1}{1.745} \right) T^{1.745} \left[ \right]_{18}^{70} \\ &\quad + 0.00485 \left( \frac{1}{1.6} \right) T^{1.6} \left[ \right]_{70}^{300} \\ &= \frac{A}{L} (27.35) \end{aligned}$$

The length of the capillary = 60 cm.

The thickness of the capillary = 0.025 cm.

The mean radius of the capillary = 0.375

$$\begin{aligned} A &= 0.025 (2 \pi \times 0.375) \\ &= 0.0589 \text{ cm}^2 \end{aligned}$$

$$\dot{Q} = \frac{0.0589 \times 27.35}{60} = 0.0266 \text{ watts}$$

This amount of heat should be dissipated through the stainless steel disc and copper rod. Since most of the temperature drop occurs in the stainless steel rod, calculation of the heat transferred through it is discussed neglecting the temperature drop in the copper rod:

$$\begin{aligned} \dot{Q} &= \frac{A}{L} \int_{1.3}^3 0.000617 T^{1.21} dT \\ &= \frac{A}{L} \times \frac{0.00617}{2.21} T^{2.21} \Big|_{1.3}^3 \\ &= \frac{A}{L} (0.0027) \end{aligned}$$

The radius of the disc = 1 cm.

The thickness of the disc = 0.25 cm.

$$A = 3.14 \text{ cm}^2.$$

$$\dot{Q} = \frac{3.14}{0.25} \times 0.0027 = 0.034 \text{ watts}$$

$$\frac{0.034}{0.0266} = 1.28$$

Thus there is sufficient cooling to get rid of the heat transferred through the capillaries.\*

#### 4. Gas-handling System

A vacuum system was constructed, using an oil vapor diffusion pump (Edwards, model E02) backed by a rotary pump (Edwards, model ED75). The minimum pressure that can be arrived at in the system is  $1 \times 10^{-5}$  mm mercury which is satisfactory for our purpose.

The temperature of the He<sup>4</sup> bath can be reduced to about 1.2°K by the help of a three-inch central pumping line. This temperature allows us to cool the sample in the bellow and outside it as low as desired for calibration. The temperature of the sample being controlled by the heaters described above.

When He<sup>3</sup> is to be used as the sample, it is pumped by a rotary pump (Welch, duo-seal model 14025), which is equipped with an oil seal

---

\* There is, moreover, additional cooling by the cold gas stream.

to prevent air from leaking in or  $\text{He}^3$  from leaking out. The  $\text{He}^3$  cylinder is mounted on the pump which can be connected to the inlet of the mercury manometer, through which the He is transferred to the bellow.

When  $\text{He}^4$  is to be used as the sample, a  $\text{He}^4$  cylinder, with a reducing valve, is connected to the inlet of the mercury manometer. The use of a pump with the cylinder is limited to  $\text{He}^3$  since it is much more expensive and it is wished to pump it back to its cylinder after all measurements have been made on it.

A sketch of the gas-handling system is shown in Fig. 7. The pressure inside the bellow is measured with the help of the mercury manometer shown in the figure. An opening to the atmosphere adds one atmosphere to the pressure of one branch of the manometer when necessary. This branch is to be 150 cms long so that pressures of about 3 atmospheres (when opened to atmospheric pressure) can be maintained. The three glass chambers (Fig. 7 - parts 11) are to be calibrated for their exact sizes with an accuracy of 0.01 ml. Their sizes are around 200, 300 and 500 ml.

The pressure in the space outside the bellow is read using a Texas Instruments fused quartz bourdon tube gauge with a range of 13.6 atmospheres.

The main part of the apparatus is now ready to be used. We encountered many problems in its construction. The apparatus had to be designed to stand the large drop of temperature from room temperature to liquid helium temperatures. This was quite difficult to achieve, for leaks kept appearing, necessitating resoldering, and sometimes rebuilding of whole parts of the apparatus. Moreover, at times, it was quite difficult to locate some of these leaks. Unfortunately, time did not permit taking any data before this thesis was written.

Fig. 6.--The main part of the apparatus:

- 1 bellow
- 2 ferroxcube
- 3 space outside the bellow
- 4 copper cell
- 5 coil
- 6 teflon spacer
- 7 germanium thermometer
- 8 liquid H<sub>2</sub> chamber
- 9,10 heaters
- 11 vacuum jacket
- 12 capillary leading to H<sub>2</sub> cylinder
- 13 radiation shields
- 14 stainless steel capillary
- 15,16 capillaries leading to He cylinders
- 17 stainless steel discs
- 18 copper rods
- 19 copper box
- 20 stainless steel cylinder

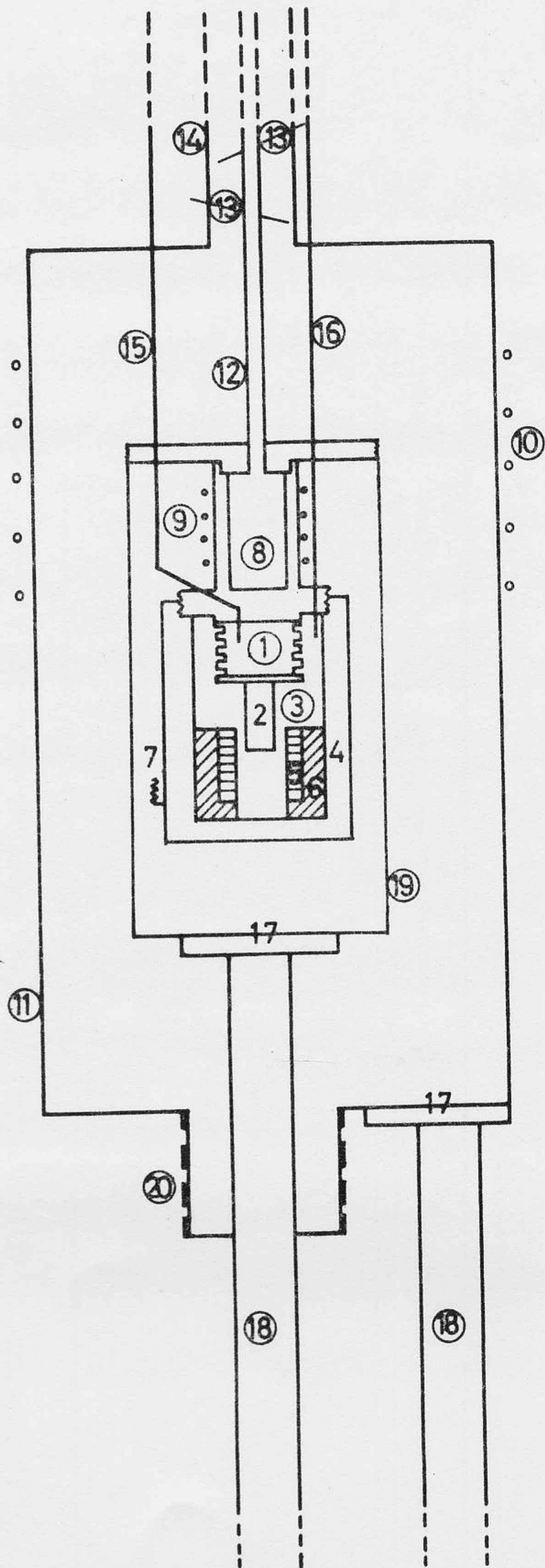
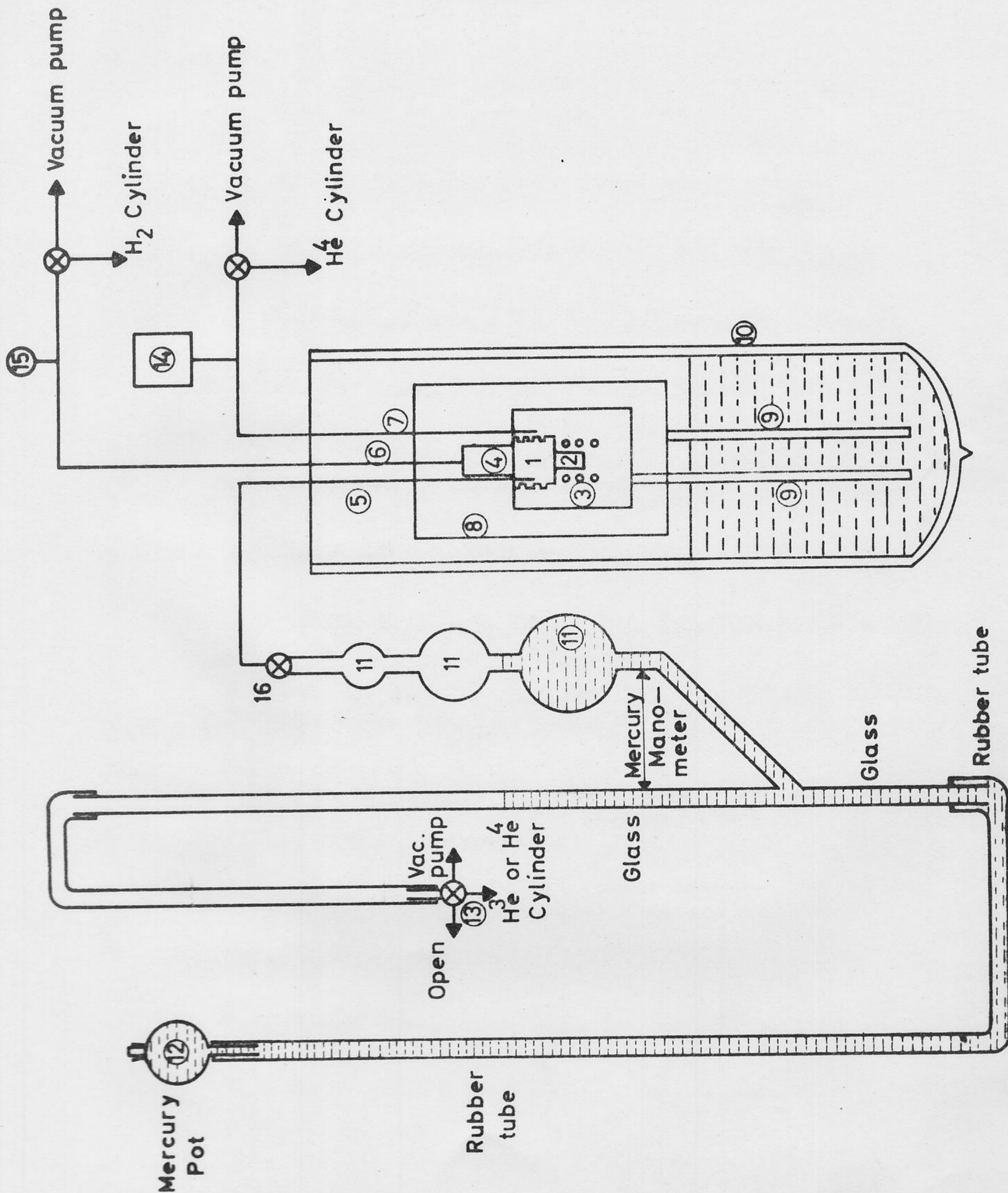


Fig. 7.--Gas-handling System

- 1 bellow
- 2 ferroxcube
- 3 coil
- 4 liquid H<sub>2</sub> chamber
- 5 capillary leading from the bellow
- 6 capillary leading from H<sub>2</sub> chamber
- 7 capillary leading from space outside the bellow
- 8 vacuum jacket
- 9 copper rods
- 10 liquid He cryostat
- 11 glass chambers
- 12 mercury pot
- 13 inlet to the mercury manometer
- 14 Texas Instruments manometer
- 15 manometer
- 16 small known-volume valve





## REFERENCES

1. C. DE LA TOUR, Ann. Chim. Phys. [2] 21, 127 (1822).
2. T. ANDREWS, Proc. Roy. Soc. (London) 18, 42 (1869).
3. T. ANDREWS, Trans. Roy. Soc. (London) A159, 575 (1869).
4. T. ANDREWS, Trans. Roy. Soc. (London) A166, 421 (1876).
5. T. ANDREWS, Trans. Roy. Soc. (London) A178, 45 (1887).
6. M.H. EDWARDS, Proceedings of the Tenth International Conference on Low Temperature Physics, Moscow, 1966 (to be published).
7. P.R. ROACH and D.H. DOUGLASS, Phys. Rev. Letters 19, 287 (1967).
8. G.O. ZIMMERMAN and C.E. CHASE, Phys. Rev. Letters 19, 151 (1967).
9. D. ELWELL and H. MEYER, American Phys. Soc. Meeting, New York, January, 1967.
10. E.C. KERR and R.H. SHERMAN, Proceedings of the Tenth International Conference on Low Temperature Physics, Moscow, 1966 (to be published).
11. M.M. EDWARDS and W.C. WOODBURY, Phys. Rev. 129, 1911 (1963).
12. M.E. FISHER, J. Math. Phys. 5, 944 (1964).
13. E.A. GUGGENHEIM, J. Chem. Phys. 13, 253 (1945).
14. M.A. WEINBERGER and W.G. SCHNEIDER, Can. J. Chem. 30, 422 (1952).
15. M.I. BAGATSKI, A.V. VORONEL' and B.G. GUSAK, Soviet Phys. - JETP 16, 517 (1963).

16. H.W. HABGOOD and W.G. SCHNEIDER, Can. J. Chem. 32, 98 (1954).
17. L.D. LANDAU and E.M. LIFSHITZ, Statistical Physics, Pergamon Press, New York (1958).
18. C.E. CHASE, R.C. WILLIAMSON and L. TISZA, Phys. Rev. Letters 13, 467 (1964).
19. L. TISZA and C.E. CHASE, Phys. Rev. Letters 15, 4 (1965).
20. L. MISTURA and D. SETTE, Phys. Rev. Letters 16, 268 (1966).
21. R.B. GRIFFITHS, Phys. Rev. Letters 16, 787 (1966).
22. M.R. MOLDOVER and W.A. LITTLE, Phys. Rev. Letters 15, 54 (1965).
23. M.E. FISHER, Phys. Rev. Letters 16, 11 (1966).
24. M.H. EDWARDS, Phys. Rev. Letters 15, 348 (1965).
25. B. WIDOM, J. Chem. Phys. 43, 3898 (1965).
26. M.J. BUCKINGHAM, Critical Phenomena, edited by M.S. Green and J.V. Sengers, National Bureau of Standards, Washington, D.C., 95 (1967).
27. R.H. SHERMAN, Phys. Rev. Letters 15, 141 (1965),
28. C.E. CHASE and G.O. ZIMMERMAN, Phys. Rev. Letters 15, 483 (1965).
29. R.H. SHERMAN and E.F. HAMMEL, Phys. Rev. Letters 15, 9 (1965).
30. C.N. YANG and C.P. YANG, Phys. Rev. Letters 13, 303 (1964).
31. J. DE BOER, Physica 14, 139 (1948).

32. L.P. KADANOFF, W. GOTZE, D. HAMBLIN, R. HECHT, E.A.S. LEWIS, V.V. PALCIAUSKAS, M. RAYL, J. SWIFT, D.ASPNES and J. KANE, Rev. Mod. Phys. 39, 395 (1967).
33. A.V. VORONEL' and M.SH. GITERMAN, Soviet Physics - JEPT 12, 809 (1961).
34. S.Y. LARSEN, R.D. MOUNTAIN and R. ZWANZIG, J. Chem. Phys. 42, 2187 (1965).
35. P.R. ROACH and D.H. DOUGLASS, Phys. Rev. Letters 17, 1083 (1966).
36. H.M. RODER, D.E. DILLER, L.A. WEBER and R.D. GOODWIN, Cryogenics 3, 16 (1965).
37. H.S. JOHNSON, W.E. KELLER and A. FRIEDMAN, J. Am. Chem. Soc. 76, 1482 (1954).
38. B. WIDOM and O.K. RICE, J. Chem. Phys. 23, 1250 (1955).
39. A.V. VORONEL', YU. R. CHASKIN, V.A. POPOV and V.G. SIMKIN, Soviet Phys. - JEIP 18, 568 (1964).
40. KH. I. AMIRKHONOV and I.G. GURVINCH, Chemical Abstracts 48, 13363g (1954).
41. H.L. LORENTZEN, Statistical Mechanics of Equilibrium and Nonequilibrium, North-Holland Publ. Co., Amsterdam (1965).
42. H.L. LORENTZEN, Acta Chem. Scand. 7, 1335 (1953).
43. S.F. ARANKI, Thesis, 1968.